AMERICAN SOCIETY FOR MICROBIOLOGY | Applied and Environmental Microbiology

Yersinia enterocolitica-Specific Infection by Bacteriophages TG1 and ϕR1-RT Is Dependent on Temperature-Regulated Expression of the Phage Host Receptor OmpF

Carlos G. Leon-Velarde,[a,f] Lotta Happonen,[i,k] Maria Pajunen,[g] Katarzyna Leskinen,[g] Andrew M. Kropinski,[b,c] Laura Mattinen,[g] Monika Rajtor,[g] Joanna Zur,[g] Darren Smith,[j] Shu Chen,[a] Ayesha Nawaz,[g] Roger P. Johnson,[d] Joseph A. Odumeru,[f] Mansel W. Griffiths,[e,f] Mikael Skurnik[g,h]

Laboratory Services Division, University of Guelph, Guelph, Ontario, Canada[a]; Department of Pathobiology, University of Guelph, Guelph, Ontario, Canada[b]; Department of Molecular and Cellular Biology, University of Guelph, Guelph, Ontario, Canada[c]; National Microbiology Laboratory at Guelph, Public Health Agency of Canada, Guelph, Ontario, Canada[d]; Canadian Research Institute for Food Safety, University of Guelph, Guelph, Ontario, Canada[e]; Department of Food Science, University of Guelph, Guelph, Ontario, Canada[f]; Department of Bacteriology and Immunology, Medicum, and Research Programs Unit, Immunobiology, University of Helsinki, Helsinki, Finland[g]; Division of Clinical Microbiology, Helsinki University Hospital, HUSLAB, Helsinki, Finland[h]; Department of Clinical Sciences Lund, Infection Medicine, Lund University, Lund, Sweden[i]; Applied Sciences, University of Northumbria, Newcastle upon Tyne, United Kingdom[j]; Institute of Biotechnology and Department of Biosciences, University of Helsinki, Helsinki, Finland[k]

ABSTRACT

Bacteriophages present huge potential both as a resource for developing novel tools for bacterial diagnostics and for use in phage therapy. This potential is also valid for bacteriophages specific for *Yersinia enterocolitica*. To increase our knowledge of *Y. enterocolitica*-specific phages, we characterized two novel yersiniophages. The genomes of the bacteriophages vB_YenM_TG1 (TG1) and vB_YenM_ϕR1-RT (ϕR1-RT), isolated from pig manure in Canada and from sewage in Finland, consist of linear double-stranded DNA of 162,101 and 168,809 bp, respectively. Their genomes comprise 262 putative coding sequences and 4 tRNA genes and share 91% overall nucleotide identity. Based on phylogenetic analyses of their whole-genome sequences and large terminase subunit protein sequences, a genus named *Tg1virus* within the family *Myoviridae* is proposed, with TG1 and ϕR1-RT (R1RT in the ICTV database) as member species. These bacteriophages exhibit a host range restricted to *Y. enterocolitica* and display lytic activity against the epidemiologically significant serotypes O:3, O:5,27, and O:9 at and below 25°C. Adsorption analyses of lipopolysaccharide (LPS) and OmpF mutants demonstrate that these phages use both the LPS inner core heptosyl residues and the outer membrane protein OmpF as phage receptors. Based on RNA sequencing and quantitative proteomics, we also demonstrate that temperature-dependent infection is due to strong repression of OmpF at 37°C. In addition, ϕR1-RT was shown to be able to enter into a pseudolysogenic state. Together, this work provides further insight into phage-host cell interactions by highlighting the importance of understanding underlying factors which may affect the abundance of phage host receptors on the cell surface.

IMPORTANCE

Only a small number of bacteriophages infecting *Y. enterocolitica*, the predominant causative agent of yersiniosis, have been previously described. Here, two newly isolated *Y. enterocolitica* phages were studied in detail, with the aim of elucidating the host cell receptors required for infection. Our research further expands the repertoire of phages available for consideration as potential antimicrobial agents or as diagnostic tools for this important bacterial pathogen.

Yersinia enterocolitica, a facultative anaerobic, Gram-negative, nonsporulating, short bacillus isolated frequently from soil, water, animals, and foods, is an important zoonotic pathogen leading to human and animal enteric infection (1). The main animal reservoir for *Y. enterocolitica* is pigs, and pork-derived products are thought to be the main source of human infections, in addition to the drinking of contaminated water and blood transfusions (1, 2). Symptoms of yersiniosis may include diarrhea, terminal ileitis, mesenteric lymphadenitis, and septicemia (3). Among the species within the genus *Yersinia*, *Y. enterocolitica* is highly heterogeneous and is grouped into six phylogroups (4). The widely used bioserotype groups form the basis of the phylogroups such that phylogroup 1 contains the biotype 1A strains, phylogroup 2 the highly pathogenic biotype 1B strains, phylogroup 3 the bioserotype 4/O:3 strains, phylogroup 4 the bioserotype 3/O:9 strains, phylogroup 5 the bioserotype 2/O:5,27 strains, and phylogroup 6 the serotype O:2,3 strains that are rarely isolated from hares (4–7). *Y. enterocolitica* is also represented by over 60 serotypes that are determined by the variability of O antigens pres-

Received 25 May 2016 **Accepted** 17 June 2016

Accepted manuscript posted online 24 June 2016

Citation Leon-Velarde CG, Happonen L, Pajunen M, Leskinen K, Kropinski AM, Mattinen L, Rajtor M, Zur J, Smith D, Chen S, Nawaz A, Johnson RP, Odumeru JA, Griffiths MW, Skurnik M. 2016. *Yersinia enterocolitica*-specific infection by bacteriophages TG1 and ϕR1-RT is dependent on temperature-regulated expression of the phage host receptor OmpF. Appl Environ Microbiol 82:5340–5353. doi:10.1128/AEM.01594-16.

Editor: H. L. Drake, University of Bayreuth

Address correspondence to Mikael Skurnik, mikael.skurnik@helsinki.fi.

Supplemental material for this article may be found at http://dx.doi.org/10.1128/AEM.01594-16.

ent in the outer cell membrane (8, 9). The predominant pathogenic strains associated with yersiniosis belong to bioserotypes 1B/O:8, 2/O:5,27, 2/O:9, 3/O:3, and 4/O:3, with the last being the most common in Europe, Japan, Canada, and the United States (1, 2). From 2010 to 2012, 98% of all reported yersiniosis infections worldwide were acquired in Europe, and most (97%) were caused by *Y. enterocolitica*, with the remainder caused by *Yersinia pseudotuberculosis* (10). In 2015, the most commonly reported *Y. enterocolitica* serotype in the European Union was O:3 (89%), followed by serotypes O:9 (7%), O:5,27 (2%), and O:8 (2%) (10).

Although several bacteriophages infecting *Y. enterocolitica* have been described, few have been studied in detail to provide reliable information on morphology, host range, and/or receptor specificity. To date, bacteriophages ϕYeO3-12 (11–13) and vB_YenP_AP5 (14) with specificity for *Y. enterocolitica* O:3, phage PY54 exhibiting a host range restricted to *Y. enterocolitica* O:5 and O:5,27 (15), *Yersinia* phage ϕR1-37 with a broad host range within the species *Y. enterocolitica* (16, 17), and *Yersinia* phage PY100 (18) exhibiting a broader host range restricted to the genus *Yersinia* have been described. These bacteriophages use different parts of the *Y. enterocolitica* lipopolysaccharide (LPS) as receptors (19). Analysis of the host range combined with genetic and structural data has shown that the receptor for ϕR1-37 is the *Y. enterocolitica* O:3 LPS outer core (OC) hexasaccharide (16). The host receptor for phages ϕYeO3-12 and vB_YenP_AP5 has been determined to be the LPS O antigen of serotype O:3, consisting of the sugar 6-deoxy-L-altropyranose (12, 14, 20). Given the interest in bacteriophages because of their potential use as therapeutic, diagnostic, and biocontrol agents, the aim of this study was to characterize two newly isolated bacteriophages that are active against several epidemiologically significant *Y. enterocolitica* serotypes. In this study, the genome characterization, morphology, host range, host cell receptor specificity, and taxonomic position of the myovirus phages vB_YenM_TG1 (here called TG1) and vB_YenM_ϕR1-RT (here called ϕR1-RT) are described.

MATERIALS AND METHODS

Bacterial strains, phage isolation, and growth conditions. Bacterial strains, bacteriophages, and plasmids are listed in Table 1. Bacteriophage ϕR1-RT was isolated from the incoming sewage of the Turku (Finland) city sewage treatment plant, as described for other viruses (19), whereas bacteriophage TG1 was isolated from pig manure collected from a rural farm in Ontario, Canada, as described previously for the isolation of *Y. enterocolitica* phages for phage typing (21). For DNA extraction and morphological studies, ϕR1-RT was propagated on *Y. enterocolitica* strain YeO3-R1 (22) and TG1 was propagated on *Y. enterocolitica* strain YeO3-c (23).

Electron microscopy. The preparation of the phage particles for transmission electron microscopy (TEM) was done as described previously (17, 24). Details are presented in the supplemental Materials and Methods.

Host range. The lytic activities of ϕR1-RT and TG1 were tested on 109 and 160 strains (see Table S1 in the supplemental material), respectively, belonging to 13 *Yersinia* species, as determined by standard spot tests (24). Briefly, 10 μl from a phage suspension containing approximately 10^8 PFU was spotted in the middle of a lawn of bacteria and incubated for 18 to 24 h. Each strain was tested three times at 25°C and at 37°C. Bacterial strains were considered sensitive to the phage if the degree of lysis was observed as a complete clearing, clearing throughout but with a faint hazy background, substantial turbidity throughout the cleared zone, or a few individual plaques (24). Bacterial strains were considered resistant if there was no effect of the phage on bacterial growth.

Genome sequencing and assembly. Details of the determination of the genomic sequences of phages ϕR1-RT and TG1 as well as the draft genomes of *Y. enterocolitica* strains YeO3-ϕR1-RT-R2, -R7, and -R9 are presented in the supplemental Materials and Methods.

Bioinformatics. A detailed description of the bioinformatics tools used is given in the supplemental Materials and Methods.

Complementation of the *Y. enterocolitica* O:3 OmpF mutant. The full open reading frame (ORF) of the *ompF* gene plus the upstream promoter region of YeO3-c was cloned as a 2-kb PCR fragment that was amplified with Phusion DNA polymerase using primer pair OmpC-F2 and OmpC-R2 (see Table S2 in the supplemental material) into plasmids pTM100 and pSW25T to obtain plasmids pTM100_OmpF and pSW25T_OmpF, respectively (Table 1). Briefly, the PCR fragments were digested with MfeI and ligated with EcoRI-digested, shrimp alkaline phosphatase-treated pTM100 or pSW25T. The constructed plasmids were mobilized to the OmpF mutant strain YeO3-c-R1-Cat17 by diparental conjugation as described earlier (25).

Phage adsorption assay. To identify the phage cell host receptors, a variety of *Y. enterocolitica* O:3 mutants (Table 1) were utilized in phage adsorption experiments. Approximately 5×10^3 PFU of phage ϕR1-RT or phage TG1 in 100 μl was mixed with a 400-μl sample of bacteria (A_{600}, ~1.2). The suspension was incubated at room temperature for 5 min and centrifuged at 16,000 × *g* for 3 min, and the phage titer remaining in the supernatant, i.e., the residual PFU percentage, was determined. LB was used as a nonadsorbing control in each assay, and the phage titer in the control supernatant was set to 100%. Each assay was performed in duplicate and repeated at least three times.

Total RNA extraction and RNA sequencing. A detailed description of the RNA extraction and sequencing methods is presented in the supplemental Materials and Methods. The RNA sequence data have been deposited in the Gene Expression Omnibus (accession number GSE66516).

Quantitative proteomics. A detailed description of the quantitative proteomics methods is presented in the supplemental Materials and Methods.

Transduction assay. *Y. enterocolitica* O:3 strain YeO3-*hfq*::Km with the *hfq* gene knocked out with a kanamycin resistance cassette (Table 1) was used as a donor, and transducing particles were produced by infecting this strain with phage ϕR1-RT by use of the soft agar overlay method. Following overnight incubation, phages were eluted from the soft agar using SM buffer (5.8 g of NaCl per liter, 2.0 g of $MgSO_4 \cdot 7H_2O$ per liter, 50 mM Tris-HCl [pH 7.5]). The transducing lysates were centrifuged and treated with chloroform to prevent contamination with the donor strain. The titer of the obtained transducing stock was 6.62×10^9 PFU/ml. *Y. enterocolitica* strain 6471/76 was used as the recipient. For the transduction of the recipient strain, 10 1-ml aliquots of log-phase bacterial cultures containing 10^9 CFU/ml cells were mixed with 100 μl of 10^{-2} diluted transducing phage stock, with a resulting multiplicity of infection (MOI) of 0.006. After 15 min, the bacterial cells were centrifuged and washed with LB and then centrifuged to remove the unabsorbed phages. The final cell pellet was resuspended in 100 μl LB, and the cells were allowed to recover during 30 min of incubation with vigorous shaking. Subsequently, the bacterial cultures were plated on urea agar plates (0.1% peptone, 0.1% glucose, 0.5% NaCl, 0.2% KH_2PO_4, 0.00012% phenol red, 2% urea, 1.5% agar) supplemented with kanamycin (200 μg/ml) and incubated for 48 h. The kanamycin-resistant and urease-negative colonies were considered transduced. The transducing stock was also plated to ensure no contamination with the donor strain.

Growth curves. Overnight bacterial cultures were diluted 1:10 in fresh LB medium, and 180-μl aliquots were distributed into honeycomb plate wells (Growth Curves Ab Ltd.), where they were mixed with 20-μl aliquots of different ϕR1-RT phage stock dilutions (10^0 to 10^{-4}). A negative control was obtained by mixing 20 μl of phage stock with 180 μl of medium, whereas the positive control consisted of 180 μl of bacterial culture and 20 μl of medium. The growth experiments were carried out at 4°C, 10°C, 16°C, 22°C, and 37°C using a Bioscreen C incubator (Growth

TABLE 1 Bacterial strains, plasmids, and bacteriophages

Strain, plasmid, or bacteriophage	Comments	Reference or source
Strains		
Y. enterocolitica		
6471/76 (YeO3)	Serotype O:3, wild type; human stool isolate	23
6471/76-c (YeO3-c)	Virulence plasmid-cured derivative of YeO3	23
YeO3-ϕR1-RT-R2	ϕR1-RT-resistant spontaneous derivative of YeO3	This work
YeO3-ϕR1-RT-R7	ϕR1-RT-resistant spontaneous derivative of YeO3	This work
YeO3-ϕR1-RT-R9	ϕR1-RT-resistant spontaneous derivative of YeO3	This work
YeO3-R1	(=YeO3-c-R1) Spontaneous rough strain	22
YeO3-*hfq*::Km	*Hfq*::Km-GenBlock, Km^r; urease negative	Leskinen et al., submitted for publication
YeO3-R1-Cat17	*ompF*::Cat-Mu derivative of YeO3-R1	This work
YeO3-R1-Cat17::pSW25T_OmpF	*cis*-complemented *ompF*::Cat-Mu strain	This work
YeO3-R1-M164	*waaF*::Cat-Mu derivative of YeO3-R1, Clm^r	79
YeO3-R1-M196	*galU*::Cat-Mu derivative of YeO3-R1, Clm^r	79
YeO3-R1-M205	*hldE*::Cat-Mu derivative of YeO3-R1, Clm^r	79
YeO3-c-OC		25
YeO3-c-OCR		25
K14	Serotype O:9	
gc815–73	Serotype O:5,27	80
8081	Serotype O:8	81
Escherichia coli		
BL21 Star (DE3) PLysS		Invitrogen
DH10B		
Plasmids		
pTM100		82
pTM100_OmpF	Complementation plasmid with wild-type *ompF* gene cloned into pTM100	This work
pSW25T	Suicide vector	83
pSW25T_OmpF	Complementation suicide plasmid with wild-type *ompF* gene cloned into pSW25T	This work
pCDF Duet-1	pCloDF13 replicon, T7lac promoter and 2 MCSs, each with an optional N-terminal His_6 tag sequence; streptomycin resistance marker	Novagen
pET21a(+)	ColE1 (pBR322) replicon, T7lac promoter, N-terminal T7 tag sequence, and optional C-terminal His_6 tag sequence; ampicillin resistance marker	Novagen
pCDF Duet-1 Gp37	Phage TG1 *ORF250* (bp 4 to 1830) cloned in frame into MCS1 of pCDF Duet-1 for expression of N-terminal His_6-tagged protein Gp37	This study
pCDF Duet-1 Gp37-Gp38	Phage TG1 *ORF251* cloned into MCS2 of pCDF Duet-1 Gp37 for coexpression of N-terminal His_6-tagged Gp37 and tail fiber assembly chaperone Gp38	This study
pET21a(+) Gp57A	Phage TG1 *ORF143* cloned into MCS of pET21a(+) for expression of general trimerization chaperone Gp57A	This study
Bacteriophages		
TG1		This study
ϕR1-RT		This study

Curves Ab Ltd.) with continuous shaking. The optical density at 600 nm (OD_{600}) of the cultures was measured at selected time intervals. The averages were calculated from values obtained for the bacteria grown in five parallel wells.

Isolation of phage-resistant mutants. A culture of wild-type *Y. enterocolitica* strain 6471/76 was used to flood LB agar plates (LA). After the excess fluid was removed, the plates were allowed to dry before two 100-μl aliquots of the ϕR1-RT stock were pipetted on the lawn of cells. The plates were incubated at 22°C and inspected daily for phage-resistant colonies growing within the lysis zones. After 3 days, several colonies appeared, and among them, three confirmed phage-resistant derivatives were isolated. The strains were named YeO3-ϕR1-RT-R2, YeO3-ϕR1-RT-R7, and YeO3-ϕR1-RT-R9.

Cat-Mu library screening. The Cat-Mu transposon insertion library in *Y. enterocolitica* strain YeO3-R1 has been described previously (26, 27). In the present work, a library representing 16,000 independent insertion mutants was screened. The library was grown in LA supplemented with 100 μg/ml chloramphenicol (LA-Clm) until an OD_{600} of ~0.5 was reached. Phage ϕR1-RT was added to 1 ml of the library culture at an MOI of ~10, fresh LB was added to achieve 5 ml, and the culture was incubated at 22°C for 2 h, during which time all phage-sensitive bacteria were expected to be infected and lysed. The surviving bacteria were pelleted by centrifugation, washed twice with 1 ml LB to remove the remaining phages, and after resuspension into 100 μl of LB, plated on four LA-Clm plates that were incubated at 22°C. The Clm^r colonies were restreaked on LA-Clm plates for further study.

Arbitrary PCR. A detailed description of the arbitrary PCR method is presented in the supplemental Materials and Methods.

Cloning, expression, and purification of the phage long-tail fiber host RBP. The phage TG1 distal long tail fiber (LTF) protein Gp37 was coexpressed with phage-encoded chaperones Gp57A and Gp38 to synthesize the native form of the putative receptor binding protein (RBP) as described previously for the LTF of phage T4 (28). The Gp37-encoding gene was first cloned into multiple cloning site (MCS) 1 of pCDF Duet-1 (conferring streptomycin resistance), producing pCDF Duet-1 Gp37. Then, the Gp38-encoding gene was cloned into the MCS 2 of pCDF Duet-1 Gp37, yielding pCDF Duet-1 Gp37-Gp38. Plasmid pET21a(+) conferring ampicillin resistance was used to clone the chaperone Gp57A-encoding gene, yielding plasmid pET21a(+) Gp57A. The plasmid constructs carry, under the control of promoter T7, high-level inducible gene expression with a His_6 fusion tag at the N terminus for purification by chelating affinity chromatography (see Fig. S1 in the supplemental material). The genes encoding Gp38 and Gp57A, however, were expressed without a purification tag. PCR, restriction analysis, and DNA sequencing were used to verify the structure of the plasmids. For expression, *Escherichia coli* BL21 Star (DE3) pLysS cells (Invitrogen) were transformed with pCDF Duet-1 Gp37 or pCDF Duet-1 Gp37-Gp38, and the same plasmids were also cotransformed with pET21a(+) Gp57A. Plasmid-bearing *E. coli* was grown aerobically at 37°C to an OD_{600} of ~0.6 with shaking at 200 rpm in 250 ml of 2× YT medium (16 g/liter tryptone, 10 g/liter yeast extract, 5.0 g/liter NaCl, 0.22-μm filter sterilized, pH 6.5 to 7.5) supplemented with 50 μg/ml of ampicillin and/or 50 μg/ml streptomycin as required. Protein expression was induced by the addition of 1 mM isopropyl-D-1-thiogalactopyranoside (IPTG) (Sigma-Aldrich, USA) and incubation for 24 h at 30°C with shaking at 200 rpm. Cells were harvested by centrifugation at 10,000 × *g* for 15 min at 4°C, and the pellets were resuspended in 25 ml of buffer A (50 mM sodium phosphate, 300 mM NaCl, 10 mM imidazole, pH 8.0) supplemented with a protease inhibitor cocktail (Roche). Cells were disrupted by 10 rounds of 15 s of sonication using a Virsonic Digital 475 ultrasonicator (VirTis, NY, USA), alternating with incubation on ice. Insoluble debris was removed by centrifugation at 18,000 × *g* for 30 min at 4°C, and the soluble fraction was filtered through a 0.22-μm-pore-size filter (EMD Millipore, USA). The protein was purified by immobilized metal ion affinity chromatography using a nickel-nitrilotriacetic acid (Ni-NTA) agarose column (Novex, Invitrogen) according to the manufacturer's protocol. Captured proteins were eluted from the column using buffer B (50 mM sodium phosphate, 300 mM NaCl, 500 mM imidazole, pH 8.0) and concentrated using Amicon-Pro centrifuge filters (Millipore) with a 10,000-Da molecular mass exclusion limit and incorporating three washes with 10 mM Tris-HCl (pH 8.5). Protein concentration was estimated by measuring sample absorbance at 280 and 260 nm using a Nanodrop 2000 UV-Vis spectrophotometer (Thermo Scientific, USA) and a Qubit protein assay kit with a Qubit 1.0 fluorometer (Life Technologies) per the manufacturer's instructions. Protein analysis was performed by sodium dodecyl sulfate-polyacrylamide gel electrophoresis (SDS-PAGE) (29) using Mini-Protean TGX stain-free precast gels (Bio-Rad Laboratories, USA) and Coomassie blue staining. Precision Plus Protein unstained standard (Bio-Rad Laboratories, Inc., Hercules, CA, USA) was used as a size marker for the molecular analysis of proteins. Analysis of protein bands and molecular weight (MW) estimates was performed using a Molecular Imager Gel Doc XR+ system (Bio-Rad Laboratories, Inc., Hercules, CA, USA) and Quantity One software (Bio-Rad Laboratories, Inc., Hercules, CA, USA). Accurate MW determinations and peptide mass fingerprinting analysis were performed via mass spectrometry (MS) at the Mass Spectrometry Facility, Advanced Analysis Centre of the University of Guelph (Ontario, Canada).

Cell decoration with bacteriophage host recognition binding proteins. Confocal laser immunofluorescence microscopy was used to visualize the binding of the phage TG1 LTF protein Gp37 to *Y. enterocolitica* by following methodology described by others (30). *Yersinia* strains grown in Trypticase soy broth (TSB) at 25°C or 37°C for 24 h were resuspended in wash buffer (50 mM Tris-HCl, pH 7.5), and 10-μl volumes were spotted onto clean glass slides. After air drying, the cells were fixed in a solution of 5% glutaraldehyde for 10 min and blocked with blocking buffer (5% bovine serum albumin [BSA] in 50 mM Tris-HCl buffer, pH 7.5) for 10 min. The slides were then incubated for 1 h in a solution containing 10 μg/ml of phage TG1 Gp37 (prepared in blocking buffer), followed by washing three times for 5 min in wash buffer. The slides were then incubated for 1 h in anti-His_6 tag (HIS.H8) mouse monoclonal antibody solution prepared in blocking buffer (1:1,000 dilution) and washed three times for 5 min with wash buffer. In a dark room, the slides were then incubated for 1 h in goat anti-mouse IgG DyLight 488 polyclonal antibody solution (1:500) prepared in blocking buffer and washed three times for 5 min with wash buffer. The slides were air dried prior to analysis. Cells were imaged using an upright Leica DM 6000B confocal laser microscope connected to a Leica TCS SP5 system. Images were collected digitally using Leica LAS AF imaging software and processed using ImageJ (31). To verify the specificity of the fluorescent signal, control samples were immunolabeled as described above, with the omission of incubation with the primary antibody. All antibodies were acquired from Pierce Scientific, USA.

Accession number(s). The complete genome sequences of *Yersinia* phages vB_YenM_TG1 and vB_YenM_ϕR1-RT were deposited in the NCBI nucleotide database (GenBank) under accession numbers KP202158 and HE956709, respectively. The RNA sequence data have been deposited in the Gene Expression Omnibus database under accession number GSE66516.

RESULTS

Phage morphology. Phages ϕR1-RT and TG1 were negatively stained and examined by TEM. Both phages exhibited a prolate head with apparent icosahedral symmetry and a tubular contractile and rigid tail showing transverse striations (Fig. 1). The average dimensions for the ϕR1-RT head are 82 ± 4 nm short edge-to-edge and 101 ± 5 nm vertex-to-vertex, and the tail, including the baseplate, is on average 130 ± 7 nm long. The average dimensions for the TG1 head are 91 ± 2 nm short edge-to-edge and 115 ± 6 nm vertex-to-vertex, and the tail, including the baseplate, is on average 129 ± 1 nm long. Collectively, these morphological features indicate that these phages belong to the *Myoviridae* family.

Host specificity. The host range of phages TG1 and ϕR1-RT were determined by testing their lytic activity on 160 and 109 strains, respectively, belonging to 13 *Yersinia* species, revealing virulence for *Y. enterocolitica* strains of serotypes O:1, O:2, O:3, O:5, O:6, O:5,27, O:7,8, and O:9 and some strains of serotype O:6,30 and O:6,31, while strains from other *Y. enterocolitica* serotypes and species within the genus *Yersinia* were resistant to phage infection (Table 2). TG1 and ϕR1-RT lysed their host when grown at 25°C but not at 37°C. Additionally, TG1 was unable to infect strains belonging to other 20 other genera (see Table S3 in the supplemental material), demonstrating that the phages' host range is restricted to *Y. enterocolitica*.

General features of the phage genomes. The genome of phage ϕR1-RT is 168,809 bp long and has a GC content of 34.5%. The genome contains 262 ORFs, of which 217 genes are carried on the reverse strand (as displayed on the genetic map) and 45 genes on the forward strand (see Fig. S2 in the supplemental material), with sizes ranging from 117 bp (with a product of 38 amino acids) to 3,738 bp (with a product of 1,245 amino acids). The genome of TG1 is smaller than that of ϕR1-RT at 162,101 bp in length but with a similarly low GC content of 34.6%. The TG1 genome also contains 262 ORFs, of which 223 genes are transcribed on the reverse strand (as displayed on the genetic map) and 39 genes on the forward strand (see Fig. S3), with sizes ranging from 114 bp

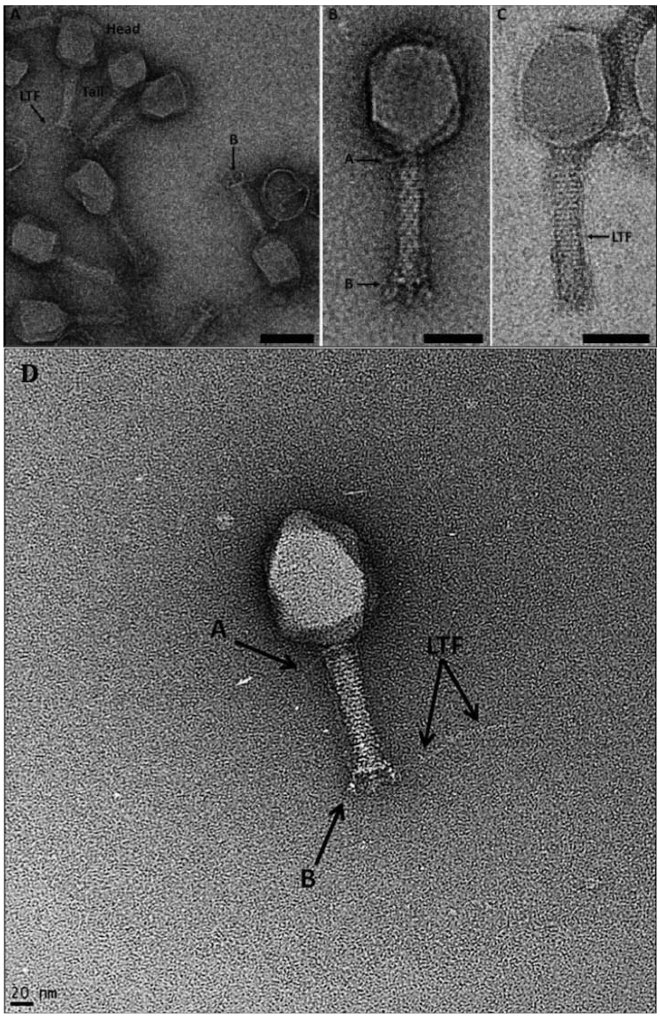

FIG 1 Electron microscopy images showing bacteriophage ϕR1-RT and TG1 morphologies. (A) ϕR1-RT virions at ×39,440 magnification. The virion head and tail are indicated, as well as long tail fibers (LTF) and a baseplate with protruding tail pins (labeled B). Scale bar, 100 nm. (B) A ϕR1-RT virion at ×84,320 magnification. A baseplate with protruding tail pins (labeled B) and a neck and collar with neck fibers (labeled A) can be observed. Scale bar, 50 nm. (C) A ϕR1-RT virion at ×108,800 magnification. Suggested LTF can be seen bent up toward the head along the tail sheath, as described for bacteriophage T4 (84). Scale bar, 50 nm. (D) Bacteriophage TG1 virion shown at ×150,000 magnification. A neck and collar with neck fibers (labeled A), a baseplate with protruding tail pins (labeled B), and an extended LTF can be observed. The scale bar indicates size in nanometers.

(with a product of 37 amino acids) to 3,099 bp (with a product of 1032 amino acids). The GC content of these phages is significantly lower than that associated with the host, which has a GC content ranging from 47.1% ± 0.2% (32) to 48.5% ± 1.5% (33). The two genomes contain the same additional four tRNA genes (Gly_{GGA}, Trp_{TGG}, Arg_{AGA}, Met_{ATG}) identified using tRNAScan (34) and ARAGORN (35). Constitutively low-GC phage genomes are often supplemented with tRNA genes that, once expressed, enhance translation efficiency when infecting high-GC-content hosts (36). At the DNA level, the TG1 genome shows 98% identity with a query coverage of 93%, for an overall DNA sequence identity of 91% with ϕR1-RT. All ORFs were screened using the BLASTP and PSI-BLAST algorithms (37, 38). Based on protein homology, putative functions could be assigned to 121 (46%) gene products of phage TG1 and 115 gene products (44%) of phage ϕR1-RT. Most of the identified homologs are conserved among T4-like phages and are either structural or involved in DNA replication, recombination, repair, or packaging. Thus, the phage T4 gene nomenclature was used to name these genes (see Table S4 in the supplemental material).

DNA replication, recombination, and repair. Numerous genes that play a direct role in DNA replication, recombination, and repair were identified within the phage ϕR1-RT and TG1 genomes. Among the genes directly involved in DNA replication are those encoding a DNA polymerase, a DNA ligase (Gp30), and three proteins with helicase activity. The closest homologs to the phage TG1 and ϕR1-RT polymerases are found in *Edwardsiella* phage PEi20 (accession number BAQ22701.1) and enterobacterial phage RB69 (NP_861746.1), all members of the *Myoviridae*. Among the helicases, Gp41 (or Dda) and UvsW homologs are involved in the reorganization of stalled DNA replication forks (39). Other putative proteins identified include homologs to the DNA polymerase sliding clamp loader complex Gp44/Gp62, sliding clamp accessory protein Gp45, single-stranded DNA binding protein Gp32, DNA helicase loader Gp59, and Gp61. In phage T4, Gp61 is a primase that interacts with helicase Gp41 to form a helicase-primase complex (or primosome). The primosome, together with the DNA helicase loader Gp59, unwinds the DNA template and primes DNA synthesis on the discontinuous strand. Among the proteins involved in recombination are type II topoisomerases Gp60 and Gp52, the recombination-related endonuclease pair Gp46/Gp47, the RecA-like recombination protein UvsX, and a single-stranded DNA binding protein, UvsY (40). Lastly, among the proteins involved in repair, a DenV homolog and several RNA ligases were identified. DenV is an N-glycosylase UV repair enzyme that excises pyrimidine dimers, the major UV lesions of DNA, while RNA ligases seal breaks in RNA and may also counteract host defense of cleavage of specific tRNA molecules (41).

Nucleotide metabolism. Class I ribonucleotide reductases are responsible for the interconversion of ribo- to deoxyribonucleotides and are represented by NrdAB or NrdEF, which require oxygen for activity, class II contains NrdJ, and the oxygen-sensitive class III is represented by NrdGH (42). In TG1 and ϕR1-RT, genes coding for the aerobic ribonucleotide reductase complex subunits NrdA, NrdB, and NrdH were identified. Additionally, NrdC genes were also located. Other genes involved in nucleotide metabolism that were identified include those encoding thymidylate synthase (*Td*), thymidine kinase (*Tk*), dNMP kinase, dCMP deaminase (*Cd*), dihydrofolate reductase (*Fdr*), dCTPase-dUTPase, and the exo-DNase (*DexA*) and endo-DNase (*DenA*). A combination of at least some of these genes is required to supplement the intracellular pool of nucleotides for phage DNA and RNA synthesis (41).

Transcription. Based on the genome maps presented (see Fig. S2 and S3 in the supplemental material), phages TG1 and ϕR1-RT present similar gene arrangements. A search for promoters based on sequence similarity to the host consensus s70 promoter TTGACA(N15-18)TATAAT with a 2-bp mismatch identified 22 probable host promoters in the phage TG1 genome and 24 probable host promoters in the ϕR1-RT genome, which probably function in early transcription (see Tables S5 and S6 in the supplemental material). Additionally, 15 of the putative host promoters are lo-

TABLE 2 Lytic activities of phages TG1 and ϕR1-RT[a]

Yersinia species	Phage-sensitive serotypes[b]	Serotypes with phage-sensitive (S) and -resistant (R) strains	Phage-resistant serotypes[c]
Y. enterocolitica	O:1 [2], O:2 [2], O:3 [16], O:5 [9], O5,27 [10], O:6 [2], O:7,8 [2], O:9 [13]	O:6,30 [1S/2R], O:6,31 [1S/1R]	O:1,2,3 [1], O:4 [1], O:4,32 [1], O:8 [14], O:10 [4], O:13 [1], O:13a,13b [1], O:13,7 [2], O13,18 [1], O:14 [1], O:20 [2], O:21 [3], O:25 [1], O:25,26,44 [1], O:26,44 [1], O28,50 [1], O:34 [1], O:35,36 [1], O35,52 [1], O:41(27),K1 [1], O41(27),42 [1], O:41(27),42,K1 [1], O:41,43 [1], O:41(27),43 [2], O:50 [1], K1 NT [2], NT [3]
Y. aleksiciae			O:16 [2]
Y. aldovae			UT [2]
Y. bercovieri			O:58,16 [2], NT [1], UT [2]
Y. frederiksenii			O:3 [1], O:16 [1], O:35 [1], O:48 [1], K1 NT [1], NT [1], UT [2]
Y. intermedia			O16,21 [1], O:52,54 [1], UT [2]
Y. kristensenii			O:3 [1], O:12,25 [1], NT [2], UT [3]
Y. mollareti			O:3 [1], O:59(20,36,7) [1], UT [2]
Y. nurmii			UT [1]
Y. pekkanenii			UT [1]
Y. pseudotuberculosis			I [2], O:1b [2], O:3 [2]
Y. rohdei			UT [2]
Y. ruckeri			NT [1], UT [5]

[a] Sensitivity was tested for 160 *Yersinia* species strains (see Table S1 in the supplemental material) at 25°C. Phage ϕR1-RT sensitivity was tested with only the 109 University of Helsinki (UH) source strains (see Table S1).
[b] The numbers of strains studied are given in brackets.
[c] NT, nontypeable and either cross-reacting or not agglutinating with *Y. enterocolitica* O:3, O:5, O:8, or O:9 antisera; UT, untyped.

cated in the same relative genomic positions within each phage genome. The genomic layout, however, makes it clear that there must be additional promoters functioning to direct the transition from host to viral metabolism. A search for phage-specific promoters using PHIRE (43) and by analysis of sequences of 100 bp in length upstream of each ORF and submitting them to MEME (44) did not yield additional promoters that could be annotated with confidence. A search for putative rho-independent transcription terminators using ARNold (45, 46) yielded 21 putative terminators in the phage TG1 genome (see Table S7 in the supplemental material) and 24 in the phage ϕR1-RT genome (see Table S8). Nevertheless, the presence of phage T4 protein homologs involved in the transcription of late genes, RegA, Gp33, and the sigma factor for late transcription Gp55, suggest that the mechanism for controlling late transcription is similarly complex (41). Likewise, the presence of repressor and translational regulatory protein homologs involved in middle and late transcription, including RegB, DsbA, Alc, MotA, and AsiA, lend further support to this suggestion.

Morphogenesis. The putative structural proteins of TG1 and ϕR1-RT are homologous to existing phage proteins of the T4 supergroup of viruses (see Table S4 in the supplemental material). Among the putative phage structural genes, the phage head is likely composed of those encoding the major capsid protein Gp23 and the phage capsid vertex protein Gp24. The prohead precursor and scaffolding proteins Gp68 and Gp67, as well as internal head proteins ipIII and ipII, were also identified. Lastly, the head portal vertex protein Gp20 that is connected to the neck and through which DNA enters during packaging and exits during infection was also identified. The whiskers and neck are composed of fibritin (*wac*) and the head completion proteins Gp13 and Gp14. The tail proteins include the tail sheath terminator Gp3, the tail completion protein Gp15, the tail sheath subunit Gp18, and the tail tube subunit Gp19. Proteins that form the baseplate wedge subunits and tail pins that then go on to associate with the central hub to form the viral baseplate include Gp5, Gp6, Gp7, Gp8, Gp9, Gp10, Gp11, Gp25, Gp27, Gp28, and Gp53. Among these, Gp5 (*ORF150*) contains a predicted bacteriophage T4-like lysozyme domain (cd00735) or phage lysozyme domain (pfam00959), which aids in penetration through the peptidoglycan layer during the initial infection process. In phage T4, Gp8 and Gp9 connect the long tail fibers (LTFs) of the virus to the baseplate and trigger tail contraction after viral attachment to a host cell, while Gp11 connects the short tail fiber (STF) protein Gp12 (*ORF159*) to the baseplate (47). The baseplate wedge subunit Gp25 forms a structural component of the outer wedge of the baseplate that has lysozyme activity, evident from the presence of a conserved gene 25-like lysozyme domain (pfam04965). Based on homology and gene synteny, the proteins forming the LTFs in TG1 and ϕR1-RT are composed of the tail fiber proximal subunit Gp34, the tail fiber connector or hinge protein Gp35, the proximal tail fiber protein Gp36, and the distal tail fiber protein Gp37 (47). A variety of chaperones or assembly catalysts involved in morphogenesis were also discovered. Head formation chaperones include the capsid vertex assembly chaperone, the prohead assembly proteins Gp21 and Gp22, and the head assembly chaperone protein Gp31. Chaperones involved in tail formation include the baseplate hub assembly proteins Gp26 and Gp51. Chaperones for tail fiber assembly include gp57A, gp57B, and Gp38.

Host cell recognition elements. In phage T4, phage tail-associated receptor-binding proteins (RBPs) Gp37 and Gp12 are necessary for host cell recognition, attachment, and initiation of infection. In the phage TG1 and ϕR1-RT genomes, *ORF250* codes for putative RBPs of 609 amino acid residues and 503 amino acid residues in length, respectively, sharing 60% overall sequence identity. These proteins also share 40% sequence identity to the distal LTF RBP of *Cronobacter* phage vB_CsaM_GAP161 (YP_006986537.1) and are homologs to the LTF RBP

Gp37 of phage T4 (AJC64544.1). An alignment of these two proteins reveals a high degree of conservation at the N terminus associated with the proximal tail fiber, as well as at the C terminus associated with host recognition (see Fig. S4 in the supplemental material). More specifically, the C-terminal 63 amino acids show 95% sequence identity. Similarly, in the phage TG1 and ϕR1-RT genomes, *ORF159* codes for the STF protein Gp12, both of which are 446 amino acid residues in length and almost identical to each other, sharing 95% overall sequence identity (see Fig. S5 in the supplemental material). These proteins are homologous to the STF protein Gp12 of phage T4 (NP_049770.1).

DNA packaging. In phage TG1, the *ORF164* and *ORF165/ORF167* genes code for the small (TerS) and large (TerL) DNA packaging subunits, respectively, of a phage terminase protein complex (or holoterminase) that initiates, drives, and terminates translocation of phage DNA into proheads (48). The homologous genes in phage ϕR1-RT are represented by *ORF165* (TerS) and *ORF166/ORF168* (TerL). Usually, *terS* and *terL* are arranged side by side, but in phages TG1 and ϕR1-RT, two ORFs homologous with *terL* are found. The proteins encoded by *ORF165* in TG1 and *ORF166* in ϕR1-RT show sequence similarity to the N terminus of the phage T4 TerL. Likewise, the proteins encoded by *ORF167* in TG1 and *ORF168* in ϕR1-RT show sequence similarity to the C terminus of phage T4 TerL. BLASTX analysis (37, 38) reveals that the *terL* gene in both phages is interrupted by a transposase (PHA02552). Additionally, during packaging, the DNA ends are also protected against host RecBCD nuclease action by Gp2, the DNA end protector protein (49) identified in phage TG1 and ϕR1-RT as the product of *ORF146*.

Homing endonucleases. Homing endonuclease genes (HEGs) are not genuine phage DNA but rather belong to intron-associated selfish DNA elements (50) and are commonly found interspersed throughout *Myoviridae* genomes (41). Among the HEGs identified in phage TG1, *ORF148* and *ORF232* exhibit similarity to shortened helix-turn-helix (HN-H) endonuclease genes, and *ORF9*, *ORF43*, and *ORF66* exhibit similarity to GIY-YIG group I intron endonuclease genes. BLASTX analysis (37, 38) reveals that the gene coding for Gp47 (recombination-related endonuclease II) is divided by *ORF66*, which contains the HEG. Likewise, the gene coding for UvsX is intersected by *ORF43*, which contains the HEG. *ORF232* also divides the *nrdA* gene. In phage ϕR1-RT, five HEGs are also found throughout the genome; of these, only *ORF148* is homologous to the helix-turn-helix (HN-H) endonuclease gene that is also located in phage TG1 between the genes coding for Gp4 and Gp53. *ORF20*, *ORF51*, *ORF163*, and *ORF234* exhibit similarity to the GIY-YIG group I intron endonuclease genes, none of which interrupt or intersect other ϕR1-RT genes.

Lysis. The final stage of the phage lytic cycle involves the degradation of the bacterial cell wall and release of progeny phages induced by the effect of a pore-producing protein, the holin, and a peptidoglycan-degrading enzyme, the endolysin (51). In TG1, *ORF127* and *ORF122* in ϕR1-RT each encode an obvious endolysin containing a bacteriophage T4-like lysozyme protein domain (pfam00959) and phage-related muramidase (COG3772). Access of the endolysin to the cell wall occurs through the presence of the holin. Holins are small phage-encoded proteins characterized by the presence of transmembrane domains (TMDs), which accumulate in the cytoplasmic membrane during infection until suddenly, at a specific time, they trigger the formation of lethal lesions, resulting in destruction of the cell wall (51, 52). A search for the TG1 and ϕR1-RT holins revealed that the putative product of their respective *ORF253* genes contains a predicted t-holin domain (pfam11031) with 70% identity to the phage holin of enterobacterial phage CC31 (accession number YP_004010117.1). The protein sequences are predicted to contain a single TMD spanning amino acids 30 to 49, as well as a large C-terminal periplasmic domain spanning the amino acid residues from position 50 to the end terminal amino acid at position 218, a characteristic bitopic topology found in the holin proteins of T4-like phages (53) Moreover, as in phage T4, the putative holin gene is separated from the endolysin gene. An additional search for *Rz* and *Rz1* genes coding for transmembrane spanins involved in the disruption of the outer membrane of the host was also conducted based on gene arrangement and membrane localization signals (54). The search revealed two candidate genes, *ORF225* and *ORF224* in phage TG1 and *ORF227* and *ORF226* in phage ϕR1-RT, homologous to phage T4 pseT.3 (*Rz*) and pseT.2 (*Rz1*), respectively. As in phage T4, the *Rz* and *Rz1* genes are adjacent to each other, arranged with overlapping stop and start codons, and in addition no part of the *Rz1* sequence is embedded within the *Rz* coding region (54). In TG1 and ϕR1-RT, *Rz* possesses a single amino-terminal TMD, and *Rz1* encodes an outer membrane lipoprotein based on the presence of a signal peptidase II (SPII) cleavage site located between amino acid residues 16 and 17, as predicted by LipoP (54, 55). Lastly, the presence of phage T4 homologs to *rI*-encoded lysis inhibition regulator membrane protein and *rIII*-encoded lysis inhibitor accessory protein in TG1 and ϕR1-RT suggest the potential for lysis inhibition (LIN) following superinfection (56, 57).

Phylogeny of TG1. It is interesting to note that very similar bacteriophages with an overall DNA sequence identity of 91% were isolated from very different locations and sources, as phages TG1 and ϕR1-RT were isolated in Canada from pig manure and in Finland from raw sewage, respectively. Moreover, less than 34% overall DNA similarity exists with their closest neighbors within the *Myoviridae* (see Table S9 in the supplemental material). The relatedness of these two phages was further explored using progressiveMauve (Fig. 2) (58, 59), CoreGenes (60, 61), which the Bacterial and Archaeal Virus Subcommittee of the International Committee on Taxonomy of Viruses (ICTV) has used extensively to compare the proteomes of viruses, and phylogenetic analysis of their whole-genome sequences (see Fig. S6) and their large terminase subunit protein sequences (Fig. 3). It is evident from phylogenetic analyses that TG1 and ϕR1-RT form a distinct taxonomic clade among their closest neighbors. Based on these observations and using a 95% DNA sequence identity as the criterion for demarcation for a species, a new genus named *Tg1virus*, with phages TG1 and ϕR1-RT (R1RT in the ICTV database) as member species, was proposed to the ICTV (approved and ratified in 2016).

Growth curves. In order to study the efficiency of phage infection at different temperatures, bacterial growth after phage infection with ϕR1-RT was measured. The host bacterial strain was grown at selected temperatures with the addition of different phage stock dilutions. Bacterial growth was followed for 3 days at 4°C, 2 days at 10°C and 16°C, and 1 day at 22°C and 37°C. Lysis of the bacterial cultures was observed at 4°C, 10°C, 16°C, and 22°C, whereas at 37°C, the bacteria were not significantly affected even with the highest initial phage concentrations (Fig. 4A). The onset time of lysis depended on the temperature and initial phage titer. At 4°C, the bacterial culture started to lyse after 56 to 60 h. At 10°C, the culture infected with the highest phage titer started to lyse after

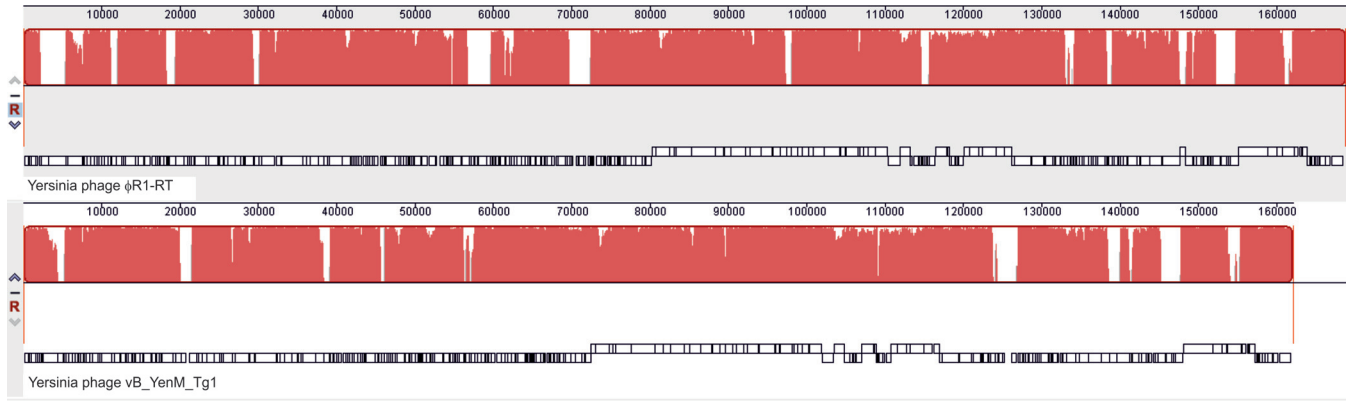

FIG 2 ProgressiveMauve alignment of phage TG1 and ϕR1-RT. The genome of ϕR1-RT (accession number HE956709) is shown at the top, and that of TG1 (accession number KP202158) is shown at the bottom of the figure. The degree of sequence similarity between regions is given by a similarity plot within the colored blocks, with the height of the plot proportional to the average nucleotide identity. Below these are illustrated the phage genes as outlined boxes on the plus (above horizontal) and minus (below horizontal) strands.

16 h, and the culture infected with the lowest phage titer started to lyse after 24 to 28 h. The corresponding times for 16°C and 22°C were 6 and 12 h. While the lysis at 10°C and 16°C was complete, at 22°C, strong regrowth took place after the initial lysis. At 4°C, the 3-day incubation time was not long enough to follow the lysis to completion. Under all tested conditions, negative (medium only) controls showed no increase in absorbance, whereas the positive (bacteria only) controls presented the normal bacterial growth pattern.

Transduction. To study the transducing potential of ϕR1-RT, transduction of the Km^r and urease-negative phenotype of strain YeO3-*hfq*::Km to the Km^s and urease-positive wild-type strain 64741/76 was assayed. Repression of urease activity is one of the phenotypes of the *hfq* mutant (62) and may be used to confirm the transduction of the *hfq*::Km allele. The transduction assays were performed in 10 parallel tubes using an MOI of 0.006. A total of 6.6×10^8 PFU from the transducing lysate resulted in a total of 3 Km^r urease-negative colonies that were confirmed by PCR. From this, the calculated transduction frequency in the experiment was 4.5×10^{-7} transductants per PFU.

Identification of the phage receptors. (i) Pseudolysogeny. As the LPS and protein profiles of the phage-resistant mutants YeO3-ϕR1-RT-2, YeO3-ϕR1-RT-7, and YeO3-ϕR1-RT-9 did not differ from those of the wild-type bacteria (data not shown), the genomic DNA of the mutant and wild-type strains were sequenced. The *de novo* assembly results showed that the total scaffold sizes of the assembled genomes of the three mutants were ~165 to 173 kb larger than that of the wild-type parental strain (see Table S10 in the supplemental material). This suggested that the mutants carry extra DNA very similar in size to the phage ϕR1-RT genome (168,809 bp). This immediately raised the possibility that the phage had lysogenized the host and would reside as a prophage. For all three draft genomes, the phage genome sequence was indeed identified, and in all it formed the fourth largest scaffold (4.1) with almost identical sizes (see Table S10). Significantly, in all three cases, the scaffold sequences were 100% identical to the phage ϕR1-RT sequence without any flanking host sequences, suggesting that the phage genome resided in these bacteria as an autonomous replicating unit in a state known as pseudolysogeny. Such a state has been described for T4-like phages (63).

(ii) Transposon insertion library screening. As selection of spontaneous phage-resistant mutants seemed to favor pseudolysogeny, we decided to use a different approach. A Cat-Mu transposon library of strain YeO3-R1 (26) was exposed to the ϕR1-RT for 2 h, and the surviving phage-resistant mutants were grown on LA-Clm plates. The recovered colonies were tested to be true ϕR1-RT-resistant mutants. In order to exclude pseudolysogens, the clones were screened with an ϕR1-RT-specific PCR, and negative ones were further analyzed by a Cat-Mu-specific arbitrary PCR to identify the Cat-Mu insertion site (26). For four of the candidates, the transposon insertion site was identified as gene *Y11_04441* of the *Y. enterocolitica* O:3 strain Y11 genome (NC_017564.1). In the strain Y11 genome, the gene was annotated to encode the outer membrane porin OmpC, but in all other *Y. enterocolitica* genomic sequences, the gene was annotated to encode OmpF, so we opted to use OmpF. To confirm that OmpF is the ϕR1-RT receptor, one of the YeO3-R1-Cat17 mutants was complemented with the wild-type *ompF* gene either in *trans* with plasmid pTM100_OmpF or in *cis* by suicide plasmid pSW25T_OmpF. Both of these approaches resulted in regaining the phage sensitivity, thus confirming that OmpF serves as the ϕR1-RT receptor.

The LPS inner core heptose region functions as a receptor. Adsorption experiments were carried out to study the ability of ϕR1-RT and TG1 to interact with *Y. enterocolitica* O:3 derivatives differing mainly in their LPS compositions (Fig. 5). A short 5-min adsorption time was used, as it produced the highest resolution between the strains. A general observation was that TG1 adsorbed faster than ϕR1-RT. Both phages showed negligible adsorption to YeO3-c-R1-Cat17, the *ompF* mutant strain, and adsorbed well to both *ompF*-complemented strains. Both phages showed reduced but clear adsorption to the pseudolysogen, indicating changes in abundance or exposure of the phage receptor(s). Finally, the adsorption to the inner core mutants decreased with the truncation of the core oligosaccharide, suggesting that the inner core heptoses are part of the secondary receptor (Fig. 5).

Temperature dependence of *ompF* expression. We then wondered whether the temperature-dependent sensitivity of *Y. enterocolitica* O:3 could be due to *ompF* regulation. The expression of *ompF* under different growth temperatures was analyzed from RNA sequencing and quantitative proteomics (liquid chromatography-tandem mass spectrometry [LC-MS/MS]) data. The tran-

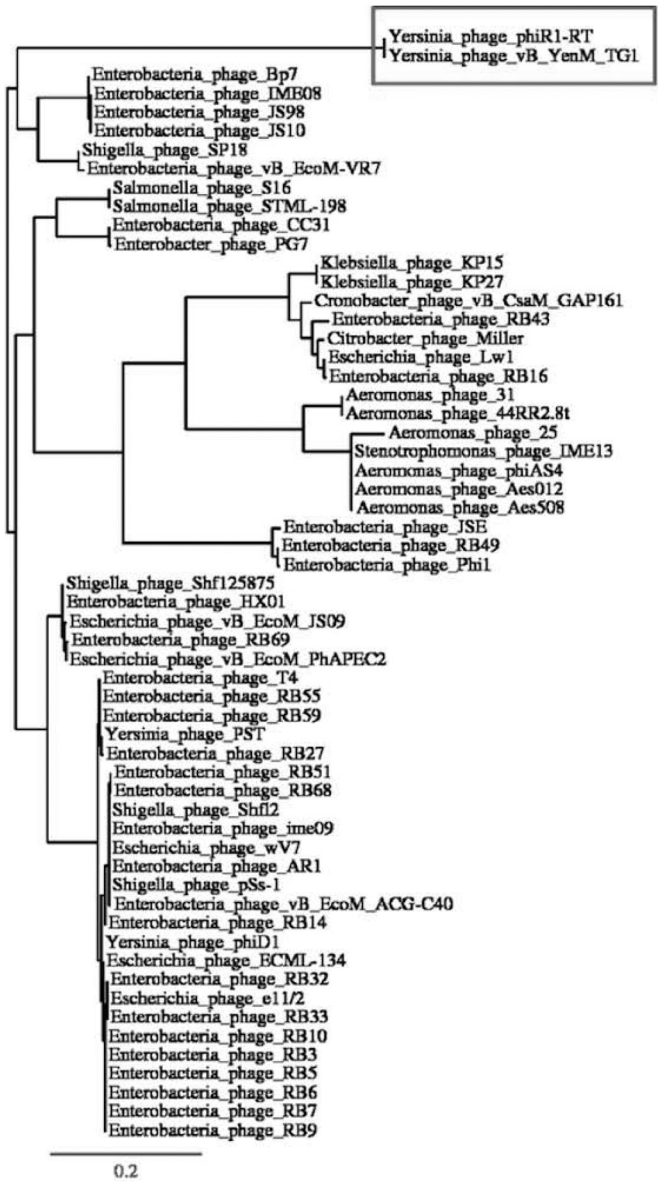

FIG 3 Phylogenetic analysis of the large terminase subunit protein sequences of phages TG1, ϕR1-RT, and related bacteriophages. The phylogenetic analysis was constructed using "one click" at phylogeny.fr (at http://phylogeny.lirmm.fr/phylo_cgi/index.cgi), with MUSCLE used for multiple alignment and PhyML used for phylogeny (85).

scriptomic data showed an inverse correlation between the expression of *ompF* and the temperature of incubation (Fig. 4B). Consistently, the quantitative proteomics demonstrated a much higher abundance of the OmpF protein in the 22°C sample than in the 37°C sample, where the abundance barely exceeded the threshold of identification (Fig. 4B).

***In vitro* expression of the LTF protein Gp37 of phage TG1.** In this study, coexpression with the phage-encoded chaperones Gp38 (required for oligomerization) and Gp57A, which is also thought to participate in assembly (64, 65), was utilized in an attempt to synthesize the native form of distal LTF protein of phage TG1, as previously described for the production of Gp37 from phage T4 (28). SDS-PAGE demonstrated that an oligomer of approximately 210 kDa was obtained when Gp37 was coexpressed with Gp38 in a bicistronic plasmid (pCDF Duet-1 Gp37-Gp38) or when this same plasmid was coexpressed with Gp57A (see Fig. S7, lanes 3 and 5, in the supplemental material). Under reduced conditions, Gp37 appears as a monomer of approximately 70 kDa in size (see Fig. S7, lanes 4 and 6). This estimate is close to the predicted molecular mass of the recombinant phage TG1 Gp37 determined via MS to be approximately 68.050 kDa. Peptide mass fingerprinting confirmed the identity of the protein (see Fig. S8). Based on the protein expression results obtained, it appears that in phage TG1, only the Gp38 chaperone is essential and the general chaperone Gp57A is not required for *in vitro* protein folding of Gp37 as has been reported for phage T4 (28). The formation of higher-molecular-weight oligomers of phage TG1 Gp37 is consistent with previous reports that describe RBPs of phages present as homotrimers in solution migrating in the SDS-PAGE with a mobility that corresponds to that of oligomeric forms (28, 66–68).

Confirmation of host binding specificity. Host binding specificity was then tested through the immunolabeling of bacterial cells with phage TG1 LTF protein Gp37, followed by detection with anti-His_6 antibodies and DyLight 488 conjugated secondary antibodies. Consistent with the temperature-dependent infection of phage TG1, the application of the LTF protein Gp37 to *Y. enterocolitica* cells showed decoration of the surfaces of *Y. enterocolitica* O:3, O:5,27, and O:9 cells when these were grown at 25°C but not at 37°C (Fig. 6). Notably, binding was more apparent near the apex of the cells, which is also reported to occur in other phages, such as λ, T4, T7, KVP40, and ϕA1122, preferentially infecting cells at the poles (69).

DISCUSSION

Among bacteriophages, the C termini of RBPs involved in ligand interactions usually exhibit considerable sequence divergence, thus providing diversity in host specificity. In the case of ϕR1-RT and TG1, the high sequence identity at the C termini of their LTF and STF proteins may account for the striking similarity in virulence of these two phages for *Y. enterocolitica*. Notably, phage ϕR1-RT shows virulence to strains of the same serotypes as phage TG1. Based on adsorption experiments, the outer membrane protein OmpF and the inner core heptosyl residues of the LPS serve as phage receptors for phage TG1 and ϕR1-RT. It is worth noting, however, that the *E. coli* strain DH10B/pTM100_OmpF was not sensitive to ϕR1-RT. We reasoned that this could be due to poor expression of *Y. enterocolitica* OmpF in *E. coli* or, more likely, that the LPS inner core, known to be used by T4-like phages as the secondary receptor (70, 71), was not compatible. The inner core structures of *E. coli* and *Y. enterocolitica* differ substantially, potentially explaining this result.

Multiple lines of evidence suggest that OmpF is the primary host range determinant for these two bacteriophages. First, a multiple alignment of OmpF amino acid sequences of *Y. enterocolitica* (from a BLASTP search of sequence databases using the O:3 OmpF sequence as the query) suggests that the restricted host range of these phages among *Y. enterocolitica* serotypes could be due to OmpF. The alignment provided a distribution of conserved amino acid residues and the presence of regions with high and low homologies, which coincide with eight transmembrane domains and eight "external" loops, respectively, of the topology of the OmpF porin from *E. coli* (72, 73). The search and alignment of the sequences (see Fig. S9 in the supplemental material) revealed that

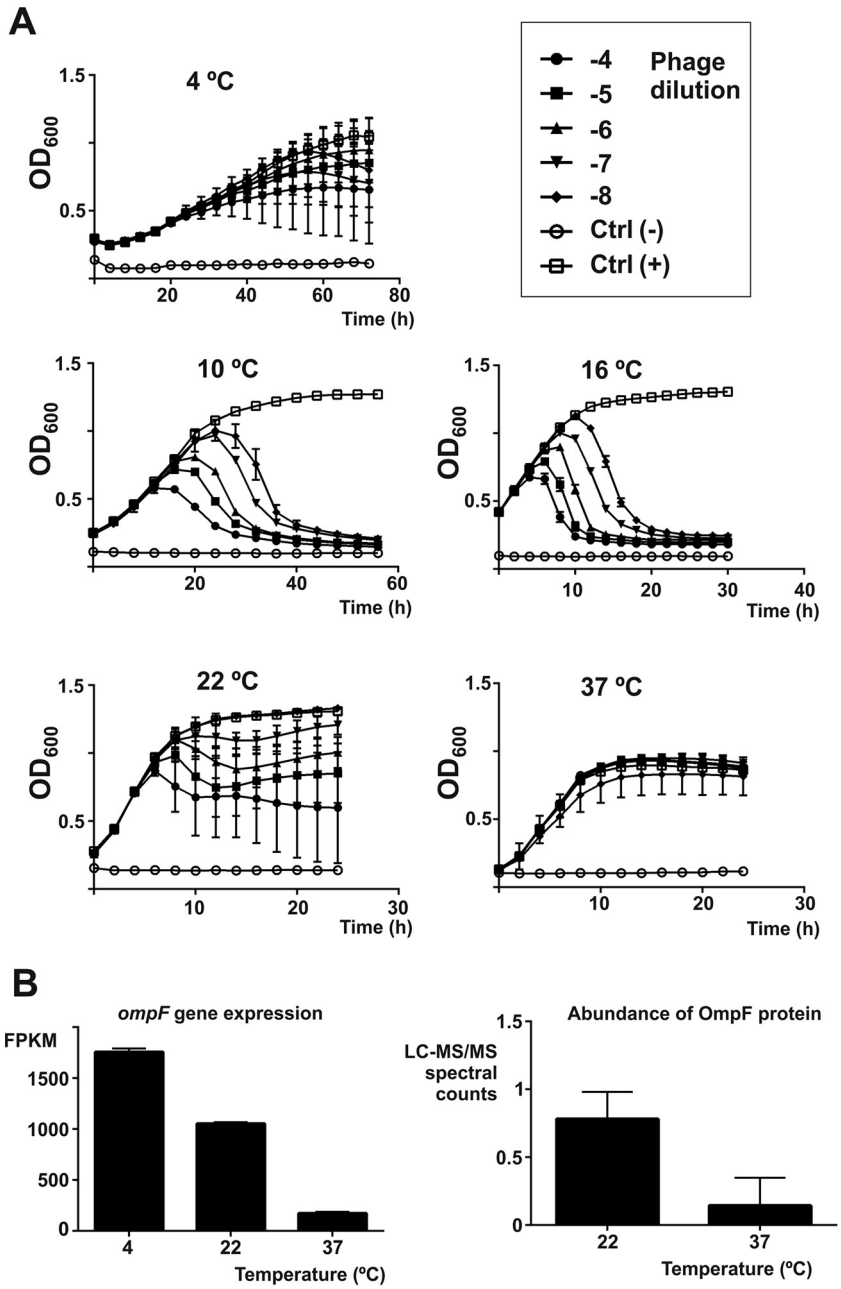

FIG 4 Phage ϕR1-RT does not propagate at 37°C. (A) Growth curves of *Y. enterocolitica* infected with ϕR1-RT. Bacteria were cultured with different concentrations of phage particles in LB at 4°C, 10°C, 16°C, 22°C, and 37°C. Each graph represents the average results for five replicates. Note the different scales used for the *x* axis at different temperatures. (B) Analysis of *ompF* gene expression (left) and protein abundance (right) at different temperatures. The mean expression levels of the *ompF* gene were obtained from RNA sequencing analysis. The production levels of the OmpF protein were obtained from normalized mean spectral values for the proteins detected by LC-MS/MS analysis. Error bars represent the calculated standard deviations.

the OmpF sequences of the ϕR1-RT-sensitive serotypes are 100% identical. The most dramatic differences between the serotypes map to loop 4. In the alignment, the closest match to the O:3 sequence is the serotype O:7,8,19 OmpF sequence, which is 96% identical to O:3 and may still be sensitive to ϕR1-RT; in it, the loop 4 sequence differs least, while in others, differences are bigger and also accumulate in other loops, mainly in loops 5, 6, and 7 (see Fig. S9). The porin loops are plausible binding sites for bacteriophages, as demonstrated by the interaction of *E. coli* OmpF and K20 phages, which bind to the L5, L6, and L7 external loops (74–76). Thus, it is likely that the loop 4 sequence is targeted by the ϕR1-RT or TG1 receptor binding proteins, but experimental evidence is necessary to confirm this. Second, RNA sequencing and quantitative proteomics data, the analysis of growth curves of *Y. enterocolitica* infected with ϕR1-RT at various temperatures (4°C to 37°C), and results of phage host range analysis conducted at 25°C and 37°C clearly indicate that the failure of ϕR1-RT and TG1 to infect *Y. enterocolitica* O:3 at 37°C is due to the strong repression of the

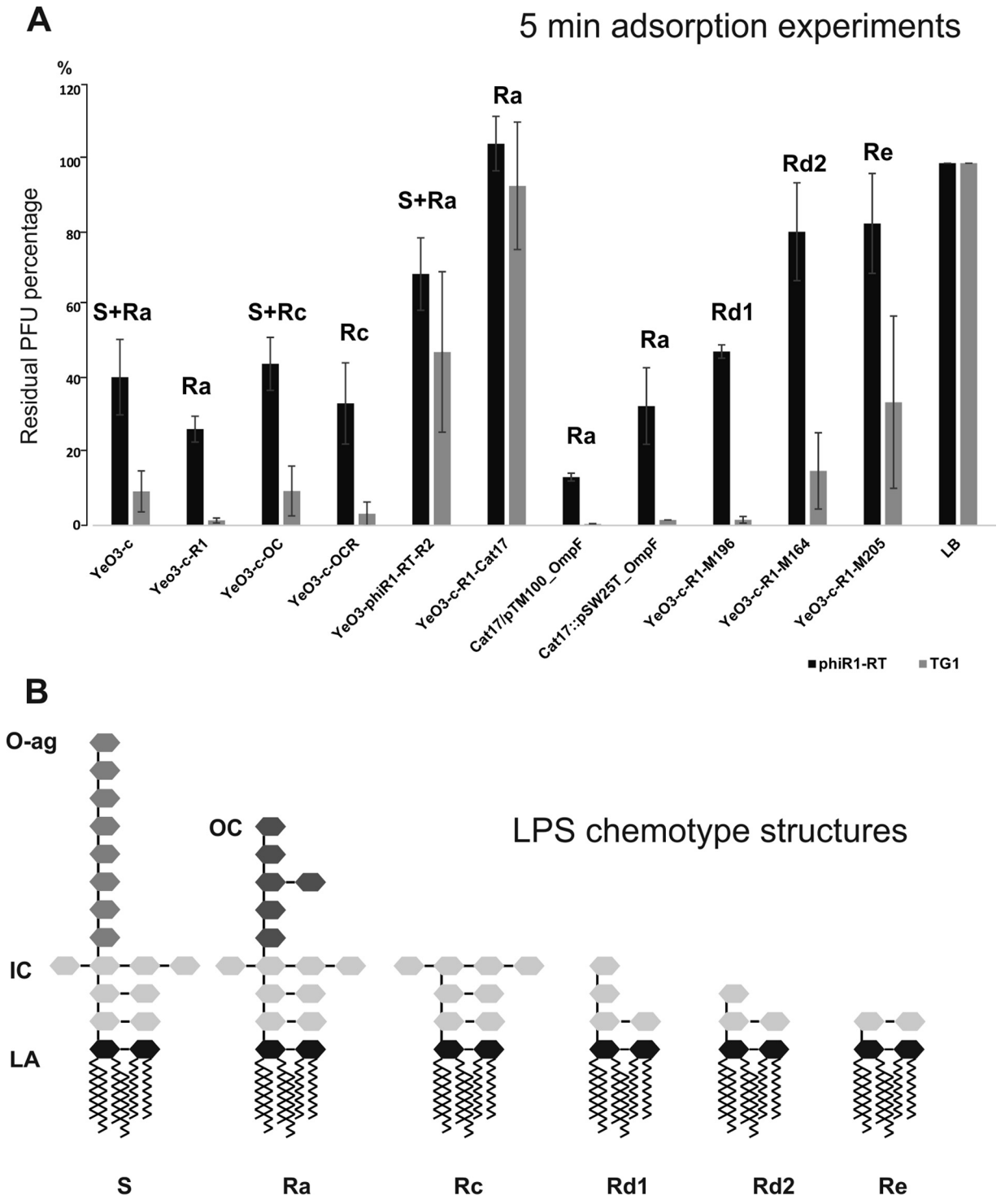

FIG 5 Phages ϕR1-RT and TG1 use OmpF and the LPS inner core heptose region of *Y. enterocolitica* O:3 as receptors. (A) Adsorption experiments were performed with different LPS and *ompF* mutants, with the complemented strains, and with the pseudolysogen. All strains are OmpF positive with the exception of YeO3-c-R1-Cat17. The TG1 and ϕR1-RT adsorptions to the bacteria at 5 min are shown as percentages of residual PFU. Error bars indicate standard deviations. The no-bacteria control (LB) and strains used for adsorptions are indicated below the columns. The LPS chemotypes of the strains are indicated at the top of the columns. (B) Schematic structures of the *Y. enterocolitica* O:3 LPS molecules of different chemotypes (86). Note that *Y. enterocolitica* O:3 carries simultaneously the S and Ra types of LPS molecules. This is indicated in panel A by a plus sign. O-ag, O-antigen or O polysaccharide; OC, outer core hexasaccharide; IC, inner core; LA, lipid A.

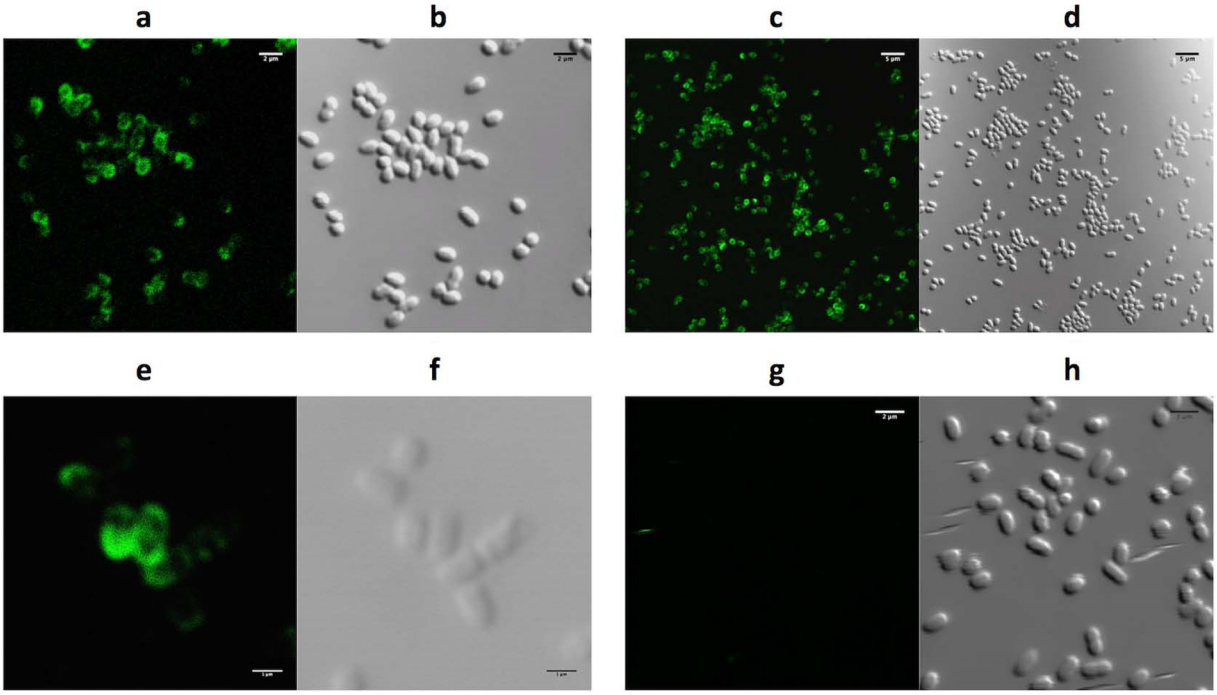

FIG 6 Confocal immunofluorescence microscopy images of *Y. enterocolitica* cells after incubation with LTF protein Gp37 derived from phage TG1. Gp37 decorates the cell surfaces of *Y. enterocolitica* strain K14 of serotype O:9 (a), *Y. enterocolitica* strain gc815-73 of serotype O:5,27 (c), and *Y. enterocolitica* strain 6471/76 of serotype O:3 (e) grown at 25°C, whereas *Y. enterocolitica* strain 8081 of serotype O:8 (g) does not show cell decoration with Gp37. Images similar to that shown in panel g were observed when the same strains were grown at 37°C. Differential interference contrast microscopy images of panels a, c, e, and g, are shown in panels b, d, f, and h, respectively. The scale bars represent sizes in micrometers.

ompF gene. The results showing the temperature-dependent expression of OmpF also agree with a previous study, where two-dimensional gel electrophoresis of whole-cell proteins of *Y. enterocolitica* cultured at 25°C and 37°C suggested that OmpF is downregulated when the bacteria were cultured at 37°C (77). Consistent with this observation, the application of immunolabeled phage TG1 receptor binding protein Gp37 to *Y. enterocolitica* cells showed decoration of the surfaces of *Y. enterocolitica* O:3, O:5,27, and O:9 cells when these were cultured at 25°C but not at 37°C. The decoration of the cell surface agrees with a high-level expression of this major outer membrane protein class, depending on the bacterial species and the environmental conditions, which can reach about $10^4$to 10^6 copies per cell (74). It is reasonable to suggest then that the phage TG1 distal LTF protein Gp37 (and by extension, its homolog in ϕR1-RT) is specifically involved in binding to OmpF while presumably the STF protein Gp12 binds to the inner core of LPS, as is reported to occur in other T even phages as a secondary receptor (70, 71).

The *in vitro* temperature-dependent infection of these two highly related phages questions their potential use as biocontrol or therapeutic agents, as has been suggested for the temperate *Yersinia* phage PY100 (18, 78). On the other hand, it is not known whether the *ompF* gene is expressed *in vivo*, justifying further studies toward finding that out. However, due to their marked specificity for the epidemiological relevant *Y. enterocolitica* serotypes O:3, O:5,27, and O:9, these phages may prove useful for diagnostic purposes. In addition, the successful synthesis of the LTF of phage TG1 opens up the possibility of its use as a probe, as well as for the production of suitable amounts of protein for X-ray crystallography to elucidate its atomic structure or cocrystallization with its receptor OmpF to shed light on specific host cell receptor-virus interactions.

ACKNOWLEDGMENTS

Karolina Grabowska and Sofia Itkonen are thanked for help in screening the Cat-Mu transposon library.

This research was supported by the Ontario Ministry of Agriculture (OMAF) Food Safety Research Program (research grant SF6075 to J.A.O.) and the Academy of Finland (grants 114075 and 288701 to M.S.).

FUNDING INFORMATION

This work, including the efforts of Carlos G. Leon-Velarde and Joseph Odumeru, was funded by Ontario Ministry of Agriculture, Food Safety Research Program (SF6075). This work, including the efforts of Mikael Skurnik, was funded by Academy of Finland (114075 and 288701).

The funders had no role in study design, data collection and interpretation, or the decision to submit the work for publication.

REFERENCES

1. **Bottone EJ.** 1999. *Yersinia enterocolitica*: overview and epidemiologic correlates. Microbes Infect **1:**323–333. http://dx.doi.org/10.1016/S1286-4579(99)80028-8.
2. **Fredriksson-Ahomaa M, Stolle A, Korkeala H.** 2006. Molecular epidemiology of *Yersinia enterocolitica* infections. FEMS Immunol Med Microbiol **47:**315–329. http://dx.doi.org/10.1111/j.1574-695X.2006.00095.x.
3. **Fukushima H, Shimizu S, Inatsu Y.** 2011. *Yersinia enterocolitica* and *Yersinia pseudotuberculosis* detection in foods. J Pathog **2011:**735308. http://dx.doi.org/10.4061/2011/735308.
4. **McNally A, Thomson NR, Reuter S, Wren BW.** 2016. "Add, stir and

reduce": *Yersinia* spp. as model bacteria for pathogen evolution. Nat Rev Microbiol **14:**177–190. http://dx.doi.org/10.1038/nrmicro.2015.29.
5. **Verhaegen J, Charlier J, Lemmens P, Delmee M, Van Noyen R, Verbist L, Wauters G.** 1998. Surveillance of human *Yersinia enterocolitica* infections in Belgium: 1967-1996. Clin Infect Dis **27:**59–64. http://dx.doi.org/10.1086/514636.
6. **Wren BW.** 2003. The yersiniae—a model genus to study the rapid evolution of bacterial pathogens. Nat Rev Microbiol **1:**55–64. http://dx.doi.org/10.1038/nrmicro730.
7. **Wauters G, Kandolo K, Janssens M.** 1987. Revised biogrouping scheme of *Yersinia enterocolitica*. Contrib Microbiol Immunol **9:**14–21.
8. **Aussel L, Therisod H, Karibian D, Perry MB, Bruneteau M, Caroff M.** 2000. Novel variation of lipid A structures in strains of different *Yersinia* species. FEBS Lett **465:**87–92. http://dx.doi.org/10.1016/S0014-5793(99)01722-6.
9. **Bruneteau M, Minka S.** 2003. Lipopolysaccharides of bacterial pathogens from the genus *Yersinia*: a mini-review. Biochimie **85:**145–152. http://dx.doi.org/10.1016/S0300-9084(03)00005-1.
10. **ECDC.** 2015. Surveillance of seven priority food- and waterborne diseases in the EU/EEA. ECDC, Stockholm, Sweden.
11. **Kiljunen S, Vilen H, Pajunen M, Savilahti H, Skurnik M.** 2005. Nonessential genes of phage phiYeO3-12 include genes involved in adaptation to growth on *Yersinia enterocolitica* serotype O:3. J Bacteriol **187:**1405–1414. http://dx.doi.org/10.1128/JB.187.4.1405-1414.2005.
12. **Pajunen M, Kiljunen S, Skurnik M.** 2000. Bacteriophage phiYeO3-12, specific for *Yersinia enterocolitica* serotype O:3, is related to coliphages T3 and T7. J Bacteriol **182:**5114–5120. http://dx.doi.org/10.1128/JB.182.18.5114-5120.2000.
13. **Pajunen MI, Kiljunen SJ, Söderholm ME, Skurnik M, Soderholm ME, Skurnik M.** 2001. Complete genomic sequence of the lytic bacteriophage phiYeO3-12 of *Yersinia enterocolitica* serotype O:3. J Bacteriol **183:**1928–1937. http://dx.doi.org/10.1128/JB.183.6.1928-1937.2001.
14. **Leon-Velarde CG, Kropinski AM, Chen S, Abbasifar A, Griffiths MW, Odumeru JA.** 2014. Complete genome sequence of bacteriophage vB_YenP_AP5 which infects *Yersinia enterocolitica* of serotype O:3. Virol J **11:**188. http://dx.doi.org/10.1186/1743-422X-11-188.
15. **Hertwig S, Klein I, Schmidt V, Beck S, Hammerl JA, Appel B.** 2003. Sequence analysis of the genome of the temperate *Yersinia enterocolitica* phage PY54. J Mol Biol **331:**605–622. http://dx.doi.org/10.1016/S0022-2836(03)00763-0.
16. **Kiljunen S, Hakala K, Pinta E, Huttunen S, Pluta P, Gador A, Lonnberg H, Skurnik M.** 2005. Yersiniophage phiR1-37 is a tailed bacteriophage having a 270 kb DNA genome with thymidine replaced by deoxyuridine. Microbiology **151:**4093–4102. http://dx.doi.org/10.1099/mic.0.28265-0.
17. **Skurnik M, Hyytiäinen HJ, Happonen LJ, Kiljunen S, Datta N, Mattinen L, Williamson K, Kristo P, Szeliga M, Kalin-Mänttäri L, Ahola-Iivarinen E, Kalkkinen N, Butcher SJ.** 2012. Characterization of the genome, proteome, and structure of yersiniophage ϕR1-37. J Virol **86:**12625–12642. http://dx.doi.org/10.1128/JVI.01783-12.
18. **Schwudke D, Ergin A, Michael K, Volkmar S, Appel B, Knabner D, Konietzny A, Strauch E.** 2008. Broad-host-range Yersinia phage PY100: genome sequence, proteome analysis of virions, and DNA packaging strategy. J Bacteriol **190:**332–342. http://dx.doi.org/10.1128/JB.01402-07.
19. **Skurnik M.** 1999. Molecular genetics of Yersinia lipopolysaccharide, p 23–51. *In* Goldberg JB (ed), Genetics of bacterial polysaccharides. CRC Press, Boca Raton, FL.
20. **al-Hendy A, Toivanen P, Skurnik M.** 1991. Expression cloning of *Yersinia enterocolitica* O:3 rfb gene cluster in Escherichia coli K12. Microb Pathog **10:**47–59. http://dx.doi.org/10.1016/0882-4010(91)90065-I.
21. **Baker PM, Farmer JJ.** 1982. New bacteriophage typing system for *Yersinia enterocolitica*, *Yersinia kristensenii*, *Yersinia frederiksenii*, and *Yersinia intermedia*: correlation with serotyping, biotyping, and antibiotic susceptibility. J Clin Microbiol **15:**491–502.
22. **al-Hendy A, Toivanen P, Skurnik M.** 1992. Lipopolysaccharide O side chain of *Yersinia enterocolitica* O:3 is an essential virulence factor in an orally infected murine model. Infect Immun **60:**870–875.
23. **Skurnik M.** 1984. Lack of correlation between the presence of plasmids and fimbriae in *Yersinia enterocolitica* and *Yersinia pseudotuberculosis*. J Appl Bacteriol **56:**355–363. http://dx.doi.org/10.1111/j.1365-2672.1984.tb01362.x.
24. **Kutter E.** 2009. Phage host range and efficiency of plating, p 141. *In* Clokie MRJ, Kropinski AM (ed), Bacteriophages: methods and protocols, vol 1. Humana Press, New York, NY.
25. **Biedzka-Sarek M, Venho R, Skurnik M.** 2005. Role of YadA, Ail, and lipopolysaccharide in serum resistance of *Yersinia enterocolitica* serotype O:3. Infect Immun **73:**2232–2244. http://dx.doi.org/10.1128/IAI.73.4.2232-2244.2005.
26. **Pinta E, Li Z, Batzilla J, Pajunen M, Kasanen T, Rabsztyn K, Rakin A, Skurnik M.** 2012. Identification of three oligo-polysaccharide-specific ligases in *Yersinia enterocolitica*. Mol Microbiol **83:**125–136. http://dx.doi.org/10.1111/j.1365-2958.2011.07918.x.
27. **Pajunen M, Kiljunen S, Skurnik M.** 2012. Construction and screening of a transposon insertion library of *Yersinia enterocolitica* (YeO3-R1). Bioprotocol **2**(15):e246.
28. **Bartual SG, Garcia-Doval C, Alonso J, Schoehn G, van Raaij MJ.** 2010. Two-chaperone assisted soluble expression and purification of the bacteriophage T4 long tail fibre protein Gp37. Protein Expr Purif **70:**116–121. http://dx.doi.org/10.1016/j.pep.2009.11.005.
29. **Laemmli UK.** 1970. Cleavage of structural proteins during the assembly of the head of bacteriophage T4. Nature **227:**680–685. http://dx.doi.org/10.1038/227680a0.
30. **Javed MA, Poshtiban S, Arutyunov D, Evoy S, Szymanski CM.** 2013. Bacteriophage receptor binding protein based assays for the simultaneous detection of *Campylobacter jejuni* and *Campylobacter coli*. PLoS One **8:**e69770. http://dx.doi.org/10.1371/journal.pone.0069770.
31. **Schneider CA, Rasband WS, Eliceiri KW.** 2012. NIH Image to ImageJ: 25 years of image analysis. Nat Methods **9:**671–675. http://dx.doi.org/10.1038/nmeth.2089.
32. **Daligault HE, Davenport KW, Minogue TD, Bishop-Lilly KA, Broomall SM, Bruce DC, Chain PS, Coyne SR, Frey KG, Gibbons HS, Jaissle J, Koroleva GI, Ladner JT, Lo C-C, Munk C, Palacios GF, Redden CL, Rosenzweig CN, Scholz MB, Johnson SL.** 2014. Whole-genome *Yersinia* sp. assemblies from 10 diverse strains. Genome Announc **2:**e01055-14. http://dx.doi.org/10.1128/genomeA.01055-14.
33. **Brenner DJ, Ursing J, Bercovier H, Steigerwalt AG, Fanning GR, Alonso JM, Mollaret HH.** 1980. Deoxyribonucleic acid relatedness in *Yersinia enterocolitica* and *Yersinia enterocolitica*-like organisms. Curr Microbiol **4:**195–200. http://dx.doi.org/10.1007/BF02605856.
34. **Schattner P, Brooks AN, Lowe TM.** 2005. The tRNAscan-SE, snoscan and snoGPS web servers for the detection of tRNAs and snoRNAs. Nucleic Acids Res **33:**W686–W689. http://dx.doi.org/10.1093/nar/gki366.
35. **Laslett D, Canback B.** 2004. ARAGORN, a program to detect tRNA genes and tmRNA genes in nucleotide sequences. Nucleic Acids Res **32:**11–16. http://dx.doi.org/10.1093/nar/gkh152.
36. **Miller ES, Kutter E, Mosig G, Arisaka F, Kunisawa T, Rüger W.** 2003. Bacteriophage T4 genome. Microbiol Mol Biol Rev **67:**86–156. http://dx.doi.org/10.1128/MMBR.67.1.86-156.2003.
37. **Altschul SF, Gish W, Miller W, Myers EW, Lipman DJ.** 1990. Basic local alignment search tool. J Mol Biol **215:**403–410. http://dx.doi.org/10.1016/S0022-2836(05)80360-2.
38. **Altschul SF, Madden TL, Schäffer AA, Zhang J, Zhang Z, Miller W, Lipman DJ.** 1997. Gapped BLAST and PSI-BLAST: a new generation of protein database search programs. Nucleic Acids Res **25:**3389–3402. http://dx.doi.org/10.1093/nar/25.17.3389.
39. **Manosas M, Perumal SK, Croquette V, Benkovic SJ.** 2012. Direct observation of stalled fork restart via fork regression in the T4 replication system. Science **338:**1217–1220. http://dx.doi.org/10.1126/science.1225437.
40. **Liu J, Morrical SW.** 2010. Assembly and dynamics of the bacteriophage T4 homologous recombination machinery. Virol J **7:**357. http://dx.doi.org/10.1186/1743-422X-7-357.
41. **Petrov VM, Ratnayaka S, Nolan JM, Miller ES, Karam JD.** 2010. Genomes of the T4-related bacteriophages as windows on microbial genome evolution. Virol J **7:**292. http://dx.doi.org/10.1186/1743-422X-7-292.
42. **Lundin D, Torrents E, Poole AM, Sjöberg B-M.** 2009. RNRdb, a curated database of the universal enzyme family ribonucleotide reductase, reveals a high level of misannotation in sequences deposited to GenBank. BMC Genomics **10:**589. http://dx.doi.org/10.1186/1471-2164-10-589.
43. **Lavigne R, Sun WD, Volckaert G.** 2004. PHIRE, a deterministic approach to reveal regulatory elements in bacteriophage genomes. Bioinformatics **20:**629–635. http://dx.doi.org/10.1093/bioinformatics/btg456.
44. **Bailey TL, Boden M, Buske FA, Frith M, Grant CE, Clementi L, Ren J, Li WW, Noble WS.** 2009. MEME SUITE: tools for motif discovery and searching. Nucleic Acids Res **37:**W202–W208. http://dx.doi.org/10.1093/nar/gkp335.

45. **Gautheret D, Lambert A.** 2001. Direct RNA motif definition and identification from multiple sequence alignments using secondary structure profiles. J Mol Biol **313:**1003–1011. http://dx.doi.org/10.1006/jmbi.2001.5102.
46. **Macke TJ, Ecker DJ, Gutell RR, Gautheret D, Case DA, Sampath R.** 2001. RNAMotif, an RNA secondary structure definition and search algorithm. Nucleic Acids Res **29:**4724–4735. http://dx.doi.org/10.1093/nar/29.22.4724.
47. **Leiman PG, Arisaka F, van Raaij MJ, Kostyuchenko VA, Aksyuk AA, Kanamaru S, Rossmann MG.** 2010. Morphogenesis of the T4 tail and tail fibers. Virol J **7:**355. http://dx.doi.org/10.1186/1743-422X-7-355.
48. **Mitchell MS, Rao VB.** 2006. Functional analysis of the bacteriophage T4 DNA-packaging ATPase motor. J Biol Chem **281:**518–527. http://dx.doi.org/10.1074/jbc.M507719200.
49. **Lipinska B, Rao AS, Bolten BM, Balakrishnan R, Goldberg EB.** 1989. Cloning and identification of bacteriophage T4 gene 2 product Gp2 and action of Gp2 on infecting DNA in vivo. J Bacteriol **171:**488–497.
50. **Bell-Pedersen D, Quirk S, Clyman J, Belfort M.** 1990. Intron mobility in phage T4 is dependent upon a distinctive class of endonucleases and independent of DNA sequences encoding the intron core: mechanistic and evolutionary implications. Nucleic Acids Res **18:**3763–3770. http://dx.doi.org/10.1093/nar/18.13.3763.
51. **Wang IN, Smith DL, Young R.** 2000. Holins: the protein clocks of bacteriophage infections. Annu Rev Microbiol **54:**799–825. http://dx.doi.org/10.1146/annurev.micro.54.1.799.
52. **Dewey JS, Savva CG, White RL, Vitha S, Holzenburg A, Young R.** 2010. Micron-scale holes terminate the phage infection cycle. Proc Natl Acad Sci U S A **107:**2219–2223. http://dx.doi.org/10.1073/pnas.0914030107.
53. **Tran TAT, Struck DK, Young R.** 2005. Periplasmic domains define holin-antiholin interactions in T4 lysis inhibition. J Bacteriol **187:**6631–6640. http://dx.doi.org/10.1128/JB.187.19.6631-6640.2005.
54. **Summer EJ, Berry J, Tran TA, Niu L, Struck DK, Young R.** 2007. Rz/Rz1 lysis gene equivalents in phages of Gram-negative hosts. J Mol Biol **373:**1098–1112. http://dx.doi.org/10.1016/j.jmb.2007.08.045.
55. **Juncker AS, Willenbrock H, Von Heijne G, Brunak S, Nielsen H, Krogh A.** 2003. Prediction of lipoprotein signal peptides in Gram-negative bacteria. Protein Sci **12:**1652–1662. http://dx.doi.org/10.1110/ps.0303703.
56. **Doermann AH.** 1948. Lysis and lysis inhibition with *Escherichia coli* bacteriophage. J Bacteriol **55:**257–276.
57. **Burch LH, Zhang L, Chao FG, Xu H, Drake JW.** 2011. The bacteriophage T4 rapid-lysis genes and their mutational proclivities. J Bacteriol **193:**3537–3545. http://dx.doi.org/10.1128/JB.00138-11.
58. **Darling AC, Mau B, Blattner FR, Perna NT.** 2004. Mauve: multiple alignment of conserved genomic sequence with rearrangements. Genome Res **14:**1394–1403. http://dx.doi.org/10.1101/gr.2289704.
59. **Darling AE, Mau B, Perna NT.** 2010. progressiveMauve: multiple genome alignment with gene gain, loss and rearrangement. PLoS One **5:**e11147. http://dx.doi.org/10.1371/journal.pone.0011147.
60. **Zafar N, Mazumder R, Seto D.** 2002. CoreGenes: a computational tool for identifying and cataloging "core" genes in a set of small genomes. BMC Bioinformatics **3:**12. http://dx.doi.org/10.1186/1471-2105-3-12.
61. **Turner D, Reynolds D, Seto D, Mahadevan P.** 2013. CoreGenes3.5: a webserver for the determination of core genes from sets of viral and small bacterial genomes. BMC Res Notes **6:**140. http://dx.doi.org/10.1186/1756-0500-6-140.
62. **Kakoschke T, Kakoschke S, Magistro G, Schubert S, Borath M, Heesemann J, Rossier O.** 2014. The RNA chaperone Hfq impacts growth, metabolism and production of virulence factors in *Yersinia enterocolitica*. PLoS One **9:**e86113. http://dx.doi.org/10.1371/journal.pone.0086113.
63. **Łoś M, Węgrzyn G.** 2012. Pseudolysogeny. Adv Virus Res **82:**339–349. http://dx.doi.org/10.1016/B978-0-12-394621-8.00019-4.
64. **Marusich EI, Kurochkina LP, Mesyanzhinov VV.** 1998. Chaperones in bacteriophage T4 assembly. Biochemistry Biokhimiia **63:**399–406.
65. **Matsui T, Griniuviene B, Goldberg E, Tsugita A, Tanaka N, Arisaka F.** 1997. Isolation and characterization of a molecular chaperone, Gp57A, of bacteriophage T4. J Bacteriol **179:**1846–1851.
66. **Garcia-Doval C, van Raaij MJ.** 2012. Structure of the receptor-binding carboxy-terminal domain of bacteriophage T7 tail fibers. Proc Natl Acad Sci U S A **109:**9390–9395. http://dx.doi.org/10.1073/pnas.1119719109.
67. **Cerritelli ME, Wall JS, Simon MN, Conway JF, Steven AC.** 1996. Stoichiometry and domain organization of the long tail-fiber of bacteriophage T4: a hinged viral adhesin. J Mol Biol **260:**767–780. http://dx.doi.org/10.1006/jmbi.1996.0436.
68. **Hashemolhosseini S, Stierhof YD, Hindennach I, Henning U.** 1996. Characterization of the helper proteins for the assembly of tail fibers of coliphages T4 and lambda. J Bacteriol **178:**6258–6265.
69. **Edgar R, Rokney A, Feeney M, Semsey S, Kessel M, Goldberg MB, Adhya S, Oppenheim AB.** 2008. Bacteriophage infection is targeted to cellular poles. Mol Microbiol **68:**1107–1116. http://dx.doi.org/10.1111/j.1365-2958.2008.06205.x.
70. **Riede I.** 1987. Receptor specificity of the short tail fibres (Gp12) of T-even type *Escherichia coli* phages. Mol Gen Genet **206:**110–115. http://dx.doi.org/10.1007/BF00326544.
71. **Thomassen E, Gielen G, Schütz M, Schoehn G, Abrahams JP, Miller S, van Raaij MJ.** 2003. The structure of the receptor-binding domain of the bacteriophage T4 short tail fibre reveals a knitted trimeric metal-binding fold. J Mol Biol **331:**361–373. http://dx.doi.org/10.1016/S0022-2836(03)00755-1.
72. **Guzev KV, Isaeva MP, Novikova OD, Solov'eva TF, Rasskazov VA.** 2005. Molecular characteristics of OmpF-like porins from pathogenic *Yersinia*. Biochemistry Biokhimiia **70:**1104–1110. http://dx.doi.org/10.1007/s10541-005-0231-z.
73. **Stenkova AM, Isaeva MP, Shubin FN, Rasskazov VA, Rakin AV.** 2011. Trends of the major porin gene (*ompF*) evolution: insight from the genus *Yersinia*. PLoS One **6:**e20546. http://dx.doi.org/10.1371/journal.pone.0020546.
74. **Achouak W, Heulin T, PagÃš J-M.** 2001. Multiple facets of bacterial porins. FEMS Microbiol Lett **199:**1–7. http://dx.doi.org/10.1111/j.1574-6968.2001.tb10642.x.
75. **Silverman JA, Benson SA.** 1987. Bacteriophage K20 requires both the OmpF porin and lipopolysaccharide for receptor function. J Bacteriol **169:**4830–4833.
76. **Traurig M, Misra R.** 1999. Identification of bacteriophage K20 binding regions of OmpF and lipopolysaccharide in *Escherichia coli* K-12. FEMS Microbiol Lett **181:**101–108. http://dx.doi.org/10.1111/j.1574-6968.1999.tb08831.x.
77. **Gu W, Wang X, Qiu H, Luo X, Xiao D, Xiao Y, Tang L, Kan B, Jing H.** 2012. Comparative antigenic proteins and proteomics of pathogenic *Yersinia enterocolitica* bio-serotypes 1B/O: 8 and 2/O: 9 cultured at 25°C and 37°C. Microbiol Immunol **56:**583–594. http://dx.doi.org/10.1111/j.1348-0421.2012.00478.x.
78. **Orquera S, Gölz G, Hertwig S, Hammerl J, Sparborth D, Joldic A, Alter T.** 2012. Control of *Campylobacter* spp. and *Yersinia enterocolitica* by virulent bacteriophages. J Mol Genet Med **6:**273–278.
79. **Noszczyńska M, Kasperkiewicz K, Duda KA, Podhorodecka J, Rabsztyn K, Gwizdała K, Świerzko AS, Radziejewska-Lebrecht J, Holst O, Skurnik M.** 2015. Serological characterization of the enterobacterial common antigen substitution of the lipopolysaccharide of *Yersinia enterocolitica* O:3. Microbiology **161:**219–227. http://dx.doi.org/10.1099/mic.0.083493-0.
80. **Kay BA, Wachsmuth K, Gemski P, Feeley JC, Quan TJ, Brenner DJ.** 1983. Virulence and phenotypic characterization of *Yersinia enterocolitica* isolated from humans in the United States. J Clin Microbiol **17:**128–138.
81. **Portnoy DA, Falkow S.** 1981. Virulence-associated plasmids from *Yersinia enterocolitica* and *Yersinia* pestis. J Bacteriol **148:**877–883.
82. **Michiels T, Cornelis GR.** 1991. Secretion of hybrid proteins by the *Yersinia* Yop export system. J Bacteriol **173:**1677–1685.
83. **Demarre G, Guérout A-M, Matsumoto-Mashimo C, Rowe-Magnus DA, Marlière P, Mazel D.** 2005. A new family of mobilizable suicide plasmids based on broad host range R388 plasmid (IncW) and RP4 plasmid (IncPalpha) conjugative machineries and their cognate *Escherichia coli* host strains. Res Microbiol **156:**245–255. http://dx.doi.org/10.1016/j.resmic.2004.09.007.
84. **Hu B, Margolin W, Molineux IJ, Liu J.** 2015. Structural remodeling of bacteriophage T4 and host membranes during infection initiation. Proc Natl Acad Sci U S A **112:**E4919–E4928. http://dx.doi.org/10.1073/pnas.1501064112.
85. **Dereeper A, Guignon V, Blanc G, Audic S, Buffet S, Chevenet F, Dufayard J-F, Guindon S, Lefort V, Lescot M, Claverie J-M, Gascuel O.** 2008. Phylogeny.fr: robust phylogenetic analysis for the non-specialist. Nucleic Acids Res **36:**W465–W469. http://dx.doi.org/10.1093/nar/gkn180.
86. **Kasperkiewicz K, Swierzko AS, Bartlomiejczyk MA, Cedzynski M, Noszczynska M, Duda KA, Michalski M, Skurnik M.** 2015. Interaction of human mannose-binding lectin (MBL) with *Yersinia enterocolitica* lipopolysaccharide. Int J Med Microbiol **305:**544–552. http://dx.doi.org/10.1016/j.ijmm.2015.07.001.